

Probing the Dipolar Coupling in a Hetero-spin Endohedral Fullerene–Phthalocyanine Dyad

Shen Zhou, Masanori Yamamoto, G. Andrew D. Briggs, Hiroshi Imahori, and Kyriakos Porfyrakis

J. Am. Chem. Soc., **Just Accepted Manuscript** • DOI: 10.1021/jacs.5b11641 • Publication Date (Web): 08 Jan 2016

Downloaded from <http://pubs.acs.org> on January 12, 2016

Just Accepted

“Just Accepted” manuscripts have been peer-reviewed and accepted for publication. They are posted online prior to technical editing, formatting for publication and author proofing. The American Chemical Society provides “Just Accepted” as a free service to the research community to expedite the dissemination of scientific material as soon as possible after acceptance. “Just Accepted” manuscripts appear in full in PDF format accompanied by an HTML abstract. “Just Accepted” manuscripts have been fully peer reviewed, but should not be considered the official version of record. They are accessible to all readers and citable by the Digital Object Identifier (DOI®). “Just Accepted” is an optional service offered to authors. Therefore, the “Just Accepted” Web site may not include all articles that will be published in the journal. After a manuscript is technically edited and formatted, it will be removed from the “Just Accepted” Web site and published as an ASAP article. Note that technical editing may introduce minor changes to the manuscript text and/or graphics which could affect content, and all legal disclaimers and ethical guidelines that apply to the journal pertain. ACS cannot be held responsible for errors or consequences arising from the use of information contained in these “Just Accepted” manuscripts.

Probing the Dipolar Coupling in a Hetero-spin Endohedral Fullerene–Phthalocyanine Dyad

Shen Zhou^{†#}, Masanori Yamamoto^{‡#}, G. Andrew. D. Briggs[†], Hiroshi Imahori^{‡§*} and Kyriakos Porfyraakis^{†*}

[†]Department of Materials, University of Oxford, OX1 3PH, UK

[‡]Department of Molecular Engineering, Graduate School of Engineering, Kyoto University, Nishikyo-ku, Kyoto 615-8510, Japan

[§]Institute for Integrated Cell-Material Sciences (WPI-iCeMS), Kyoto University, Nishikyo-ku, Kyoto 615-8510, Japan.

Endohedral Fullerene, Phthalocyanine, Electron Spin Dipolar Coupling, Aggregation, Quantum Information Processing

ABSTRACT: Paramagnetic endohedral fullerenes and phthalocyanine (Pc) complexes are promising building blocks for molecular quantum information processing, for which tunable dipolar coupling is required. We have linked these two spin qubit candidates together, and characterized the resulting electron paramagnetic resonance properties, including the spin dipolar coupling between the fullerene spin and the copper spin. Having interpreted the distance-dependent coupling strength quantitatively, and further discussed the antiferromagnetic aggregation effect of the CuPc moieties, we demonstrate two ways of tuning the dipolar coupling in such dyad systems: changing the spacer group and adjusting the solution concentration.

INTRODUCTION

Endohedral fullerenes are molecular carbon cages incarcerating heteroatoms.^{1–7} Paramagnetic fullerenes such as N@C₆₀, Sc@C₈₂, Y@C₈₂ and La@C₈₂, have relatively long electron spin relaxation times,^{8,9} making them candidates for building a molecular quantum computer.^{10–14} Significant progress has been achieved to-date in both theoretical designs, like the proposals of qubit gates^{15–17} and experimental implementations, such as robust phase gates.¹⁸ Realization of a two-qubit gate based on the electron spin with a molecular system remains challenging,^{19,20} and requires a multi-spin system with a tunable dipolar coupling effect that could be used to fabricate a two-qubit gate.

Previous studies of multi-spin endohedral fullerenes have observed electron spin dipolar coupling in N@C₆₀–CuTPP dyad,²¹ FSc₃C₂@C₈₀–PNO[•]²² and N@C₆₀–N@C₆₀ dimer.²³ The detailed properties of the dipolar coupling in these endohedral fullerene systems were not fully revealed for various reasons. For the N@C₆₀–CuTPP dyad, the spin signal from the fullerene molecule was completely suppressed by the CuTPP moiety because of the very strong coupling between the spins. In FSc₃C₂@C₈₀–PNO[•], the complicated hyperfine interaction from the three non-equivalent Sc (I_{Sc}=7/2) atoms made the spectra difficult to interpret, and obscured any effect of dipolar coupling. Studies of dipolar coupling in a N@C₆₀–N@C₆₀ di-

mer have been limited by the purity of N@C₆₀. The broad and weak dipolar coupling signal was masked by the sharp and intense signal originated from the half-filled dimer that was also present.

We have designed and synthesized a series of hetero-spin systems of endohedral fullerene–phthalocyanine dyads. Three main improvements in the molecular design enable us to overcome the limitations listed above: 1) the longer spacer groups between the spin centers avoid the complete suppression phenomenon; 2) We use N@C₆₀, which has sharper spin signal than Sc₃C₂@C₈₀, as the probing spin to simplify spectral interpretation; 3) the hetero-spins resonating at different magnetic fields solve the overlapping problem without having to use 100% pure N@C₆₀. Since CuPc has also been suggested as a promising spin qubit candidate,^{24,25} the combination of two different spin-qubits offers extra possibilities.

We have comprehensively characterized the dipolar coupling effect in the endohedral fullerene–CuPc dyad system for the first time. By comparing the spectral features of dyads having different spin distances, we show that changing the spacer group enables the tuning of the dipolar coupling strength in this system. Utilizing the aggregation and antiferromagnetism of the CuPc moiety, we further demonstrate that the concentration of the sample can also be used to influence the coupling strength in a controllable manner.

RESULTS AND DISCUSSION

Synthesis and characterization

Three different $N@C_{60}$ -phthalocyanine dyads ($N@C_{60}$ -1-CuPc, $N@C_{60}$ -2-CuPc and $N@C_{60}$ -1-ZnPc) were synthesized by reacting spin enriched $N@C_{60}/C_{60}$ mixture (1%) with corresponding phthalocyanine aldehyde through the 1,3-dipolar cycloadditions shown in Figure 1, respectively.²⁶⁻²⁸ In order to protect the endohedral fullerene (derivative) which has limited thermal,²⁹ irradiative³⁰ and chemical stability,³¹ we performed the reactions in mild conditions with a compromise on the conversion ratio. The reagents in stoichiometric ratio dissolved in toluene were refluxed for two hours in the dark. The product dyads were then isolated from the reaction mixture by high performance liquid chromatography (HPLC) through a Buckyprep-M column. Figure 2 (a) shows a representative HPLC trace for the separation of $N@C_{60}$ -1-CuPc. Although the yield of the product was relatively low (c.a. 22% based on the integrated area percentage of the product peak to the whole HPLC curve), the unreacted reagents were collected and reused for a second reaction batch to improve the overall conversion ratio to higher than 40%. Apart from the dyads, a pyrrolidine functionalized fullerene (F- C_{60} , structure shown in Supporting Information S1) was also prepared according to the literature,³² and was applied as the UV-Vis reference.

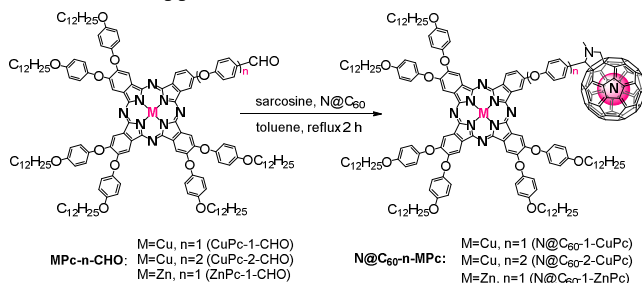


Figure 1. Synthesis of $N@C_{60}$ -phthalocyanine dyads. M represents the copper or zinc ion, and n stands for the number of the phenoxy groups in the bridging unit.

The successful formation of the products is manifested by UV-Vis absorption spectroscopy and mass spectrometry (MS). As depicted in Figure 2 (b), the spectrum for the toluene solution of $N@C_{60}$ -1-CuPc (solid line) is a superposition of the absorption features of the phthalocyanine aldehyde (dashed line) and functionalized fullerene reference (dotted line), which suggests the existence of both the phthalocyanine and fullerene moieties in the product molecule. In addition, the characteristic absorption band at 430 nm indicating the 1,2--adduct structure of the fullerene^{28,33} has also been observed in the spectrum. The MS characterization for $N@C_{60}$ -1-CuPc is shown in Figure 2 (c), where the experimental peaks (back) are consistent with the combination of the theoretical prediction of C_{60} -1-CuPc (blue) and $N@C_{60}$ -1-CuPc (red). Due to the 1% concentration of the endohedral fullerene and the potential fragmentation during the ionization, the dominant peaks are due to the empty cage dyad, but the weak MS peaks representing the endohedral fullerene dyad remains

detectable and agrees nicely with the theoretical predictions. UV/Vis and MS characterization data were also obtained for $N@C_{60}$ -2-CuPc and $N@C_{60}$ -1-ZnPc (Supporting Information S2).

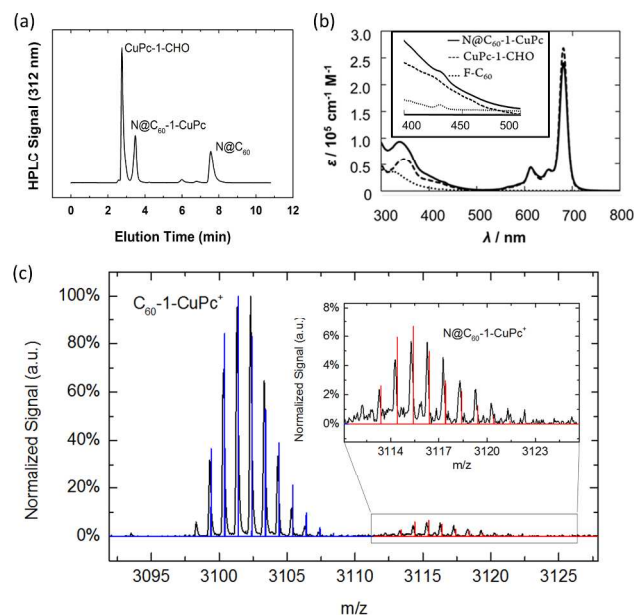


Figure 2. (a) HPLC curve for the separation of $N@C_{60}$ -1-CuPc (Buckyprep-M column, toluene, room temperature, 16 ml/min flow rate) (b) UV-Vis absorption spectrum for the toluene solution of $N@C_{60}$ -1-CuPc (solid line), which is similar to the superposition of those of phthalocyanine aldehydes (dashed line) and functionalized fullerene reference (dotted line). (c) High resolution MALDI-TOF mass spectrum of $N@C_{60}$ -1-CuPc in dithranol matrix at positive mode with the theoretical predictions. The dominant peaks are from the empty cage dyad (blue lines), but the weak MS peaks representing the endohedral fullerene dyad (red lines) are also detectable.

Analysis of the electron spin properties

We applied continuous wave electron paramagnetic resonance (CW-EPR) to study the spin properties of the synthesized dyads. Among the three dyads, $N@C_{60}$ -1-CuPc and $N@C_{60}$ -2-CuPc are multi-spin systems, while $N@C_{60}$ -1-ZnPc contains just one electron spin center. $N@C_{60}$ and CuPc, which contain the $^4S_{3/2}$ state of the endohedral nitrogen atom and the $3d^9$ electron configuration of the central Cu^{2+} ion, respectively, are spin active whereas ZnPc is spin-silent. Compared with $N@C_{60}$ -1-ZnPc, the spin signals from the multi-spin dyads are more complicated. Fortunately, as the full-range spectrum of $N@C_{60}$ -1-CuPc shows in Figure 3 (a), the signals from the copper spin and the endohedral nitrogen spin do not overlap, which enables us to interpret them separately. Herein, we mainly focused on the electron spin of $N@C_{60}$ moiety rather than that of CuPc, because of better sensitivity of its sharp signal and its higher relevance to spin-spin interaction. Limited by the purity of $N@C_{60}/C_{60}$ mixture, all dyad samples contain only 1% of $N@C_{60}$ spins but 100% of CuPc spins. Hence, 99% of CuPc spins are just covalently linked

with empty cages, whereas all $N@C_{60}$ spins are coupled with the CuPc spins.

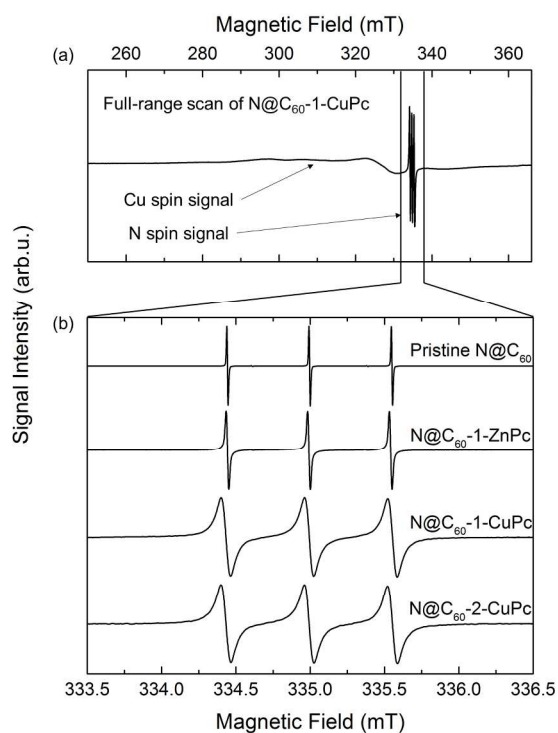


Figure 3. (a) Solution CW-EPR spectra of $N@C_{60}$ -1-CuPc (full-range) highlighting the fact that the spin signals of Cu and N do not overlap. (b) Solution CW-EPR spectra comparison of pristine $N@C_{60}$, $N@C_{60}$ -1-ZnPc, $N@C_{60}$ -1-CuPc and $N@C_{60}$ -2-CuPc, which focuses on the nitrogen spin region (all measurements were taken with 10^{-5} M toluene solution samples at room temperature).

The zoomed-in solution CW-EPR spectra of the nitrogen spin region (Figure 3 (b)) were studied first. For pristine $N@C_{60}$, $N@C_{60}$ -1-ZnPc, $N@C_{60}$ -1-CuPc and $N@C_{60}$ -2-CuPc dissolved in toluene (10^{-5} M), we obtained the same triplet patterns which are attributed to the hyperfine coupling (HFC) between the nitrogen electron spin ($S=3/2$) and nitrogen nuclear spin ($I=1$). The absence of any extra spectral splitting in the dyad spectra leads to two conclusions: 1) the molecules tumble rapidly in their respective toluene solutions, so that all anisotropic spin features having a traceless tensor, such as the potential zero-field splitting (ZFS) peaks and electron spin dipolar coupling features, are averaged-out to zero; 2) there is no discernable electron spin-spin exchange coupling in either of the multi-spin dyads, due to the near-perfect protection of the fullerene cage that excludes the probability of any spin density overlapping.²¹ Such an exotic phenomenon is different from other diradical molecular systems³⁴⁻³⁶ having similar spin separations but showing exchange coupling splitting in their solution spectra.

In contrast to the similarity on the spectral splitting pattern, the linewidth, which is inversely proportional to the relaxation time, varies, providing us with a qualitative approach to compare the relaxation time difference of the electron spin for each compound. The averaged peak-to-

peak linewidth (ΔH_{pp}) for pristine $N@C_{60}$ is measured to be less than 3 μ T, representing a ultra-long relaxation time, consistent with previous reports.⁸ The averaged ΔH_{pp} of $N@C_{60}$ -1-ZnPc is slightly broadened, resulting from the degradation of the high molecular symmetry,³⁷ the relatively lower tumbling rate³⁸ and the proton nuclear influence,³⁹ but it is still as sharp as 18 μ T. When it comes to the multi-spin molecules, $N@C_{60}$ -1-CuPc and $N@C_{60}$ -2-CuPc, the signal becomes substantially broader, with the averaged ΔH_{pp} being increased to 60 μ T and 63 μ T, respectively. Since physically mixing $N@C_{60}$ with CuPc does not show such a significant broadening effect, even at very high concentrations (supporting information S3), this phenomenon is attributed to the chemical linkage of two spin centers, which decreases the relaxation time of the endohedral spin considerably due to strong intramolecular electron spin interaction. Since the electron spin exchanged coupling has been ruled out in the splitting pattern analysis, the electron spin dipolar coupling has to be the major intermolecular spin interaction mechanism.

Having established the existence of dipolar coupling, we went on to measure the solid-state CW-EPR spectra, which allow us to extract more information on the electron spin dipolar coupling strength, by immersing the sample tube in liquid nitrogen and stabilizing the measurement conditions at 100 K with a nitrogen-flow cryostat. Benefiting from the well-controlled reaction conditions, all solid-state spectra of pristine $N@C_{60}$, $N@C_{60}$ -1-ZnPc, $N@C_{60}$ -1-CuPc and $N@C_{60}$ -2-CuPc have excellent signal-to-noise ratios, and are free of the commonly reported $S=1/2$ impurity in the functionalized $N@C_{60}$ powder spectra.^{40,41} The nitrogen spin region of the respective spectra is shown in Figure 4.

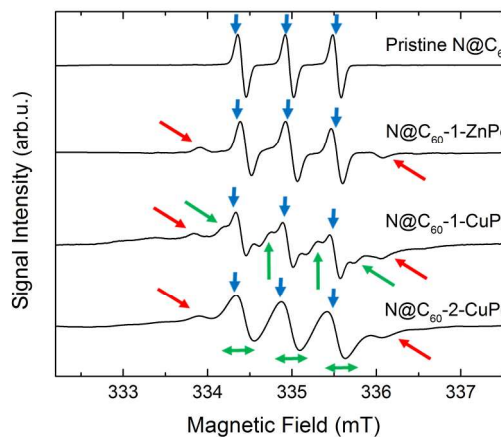


Figure 4. Solid-state CW-EPR spectra (nitrogen spin region) for pristine $N@C_{60}$, $N@C_{60}$ -1-ZnPc, $N@C_{60}$ -1-CuPc and $N@C_{60}$ -2-CuPc, respectively. All measurements were taken with 10^{-5} M frozen toluene solutions at 100 K. The peaks of hyperfine coupling (HFC) and zero-field splitting (ZFS) are labeled with blue and red arrows, respectively. The dipolar coupling features, such as fine shoulder peaks and line-broadening, are marked with green arrows.

The solid-state CW-EPR spectrum of pristine N@C₆₀ only shows three HFC peaks, which commonly exist in all spectra (indicated by blue arrows). The absence of any extra splitting results from the I_h symmetry of the fullerene cage and the effective dilution of the toluene matrix in amorphous form. In comparison, N@C₆₀-1-ZnPc having a lower molecular symmetry shows characteristic weak and broad ZFS side peaks (marked by red arrows). According to the spectrum simulation (Supporting Information S4), the axial ZFS parameter D was determined to be 14.2 MHz, which is typical for N@C₆₀ pyrrolidine derivatives. The evenly sized HFC peaks as well as the simulated isotropic HFC constant (A_{iso}=15.4 MHz) confirm that the HFC remains isotropic, providing further experimental evidence on the influence of functionalization of pyrrolidine addends on HFC. There are contradictory reports about this in the literature.^{38,41}

The spectra of N@C₆₀-1-CuPc and N@C₆₀-2-CuPc in the nitrogen spin region appear different from that for N@C₆₀-1-ZnPc (see fine features marked by green arrows), even though all these three molecules should have very similar ZFS and HFC features due to the nearly-identical structure and electron configuration in the fullerene moiety. We ascribe both of the additional fine features to the variant electron spin dipolar coupling effects, which has been shown to be the major intramolecular spin interaction by the above solution CW-EPR study. However, the fine features of the dipolar coupling in the two spectra still vary. The spectrum of N@C₆₀-1-CuPc has more obvious splitting with shoulder peaks emerging next to the HFC peaks, whereas the spectrum of N@C₆₀-2-CuPc shows broadened HFC peaks only. We attribute such splitting variation as follows: The extent of the splitting is proportional to the coupling strength,⁴² and the dipolar coupling strength is reciprocally proportional to the cube of the spin-spin varies as 1/r³ in the model in Figure 5 (a). According to the calculated spin density distributions and preferential configurations for the multi-spin dyads (Figure 5 (b) and (c)), we theoretically estimated that the separations between the spin centers are 16.65 Å (N@C₆₀-1-CuPc) and 20.96 Å (N@C₆₀-2-CuPc). Subsequently, we further determined that the coupling strength for N@C₆₀-1-CuPc (11.2 MHz) is twice as much as that for N@C₆₀-2-CuPc (5.6 MHz), which qualitatively explained the splitting variation in their spectra. To the best of our knowledge, this is the first comparison between the solid-state spectra of two variably distanced endohedral fullerene multi-spin systems. In addition, we have demonstrated experimentally the chemical tunability of the dipolar coupling strength between the potential spin qubits N@C₆₀ and CuPc by changing the length of the bridging unit between them.

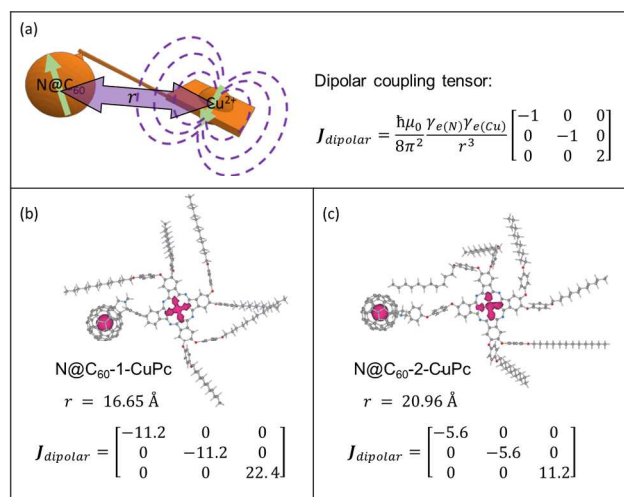


Figure 5. (a) Illustration and equation of the electron spin dipolar coupling depending on spin separation. (b) (c) The spin density distributions of the multi-spin dyads in their corresponding preferential configurations (contour levels are 1×10^{-3} e/au), based on which the electron spin distances and dipolar coupling strength were calculated, respectively.

Explanation for the low coupling strength

Despite the successful qualitative interpretation of the dipolar splitting, a quantitative one remains far more challenging. With a comprehensive spin Hamiltonian model covering the tensor value and direction, the initial simulation details are described in supporting information S5. The experimental spectra have less prominent dipolar coupling features than the simulated ones. We estimate that the apparent dipolar coupling strengths in the experimental data are c.a. 30% weaker than the theoretical predictions of 11.2 MHz and 5.6 MHz for the two multi-spin dyads. The reason for such deviations is discussed below.

The first reason one may argue is the presence of thermal vibrations for the preferential conformation. Since all distances we used for the fittings were based on DFT calculations which are optimized at 0 K whereas the experimental data were measured at 100 K, thermal vibrations might lead to larger spin separations in both dyads, which would consequently lower the resulting coupling strength. However, according to the dynamic MM2 simulation, the dyad molecules vibrate insignificantly due to the relatively rigid molecular structure. We have shown that the simulation model is insensitive to any potential error existing in the relative angle caused by the sp³ bond rotation (supporting information S8-A). Moreover, the unchanged CW-EPR spectra for both dyads, when we decreased the measurement temperature down to 77 K, also suggests that the temperature does not play a crucial role in spectral deviations. Hence the fitting failure cannot be due to the thermal vibrations of the preferential conformation.

Another potential explanation could be the magnetic shielding effect of the fullerene cage, because the ring-current effect of the π conjugated electrons on the fullerene cage is capable of partial shielding of the dipolar

magnetic field experienced by the endohedral spin. However, based on the shielding effect reported previously (6 ppm for $^3\text{He}@C_{60}$ vs. free ^3He ,⁴³ and 19 ppm for $\text{N}@C_{70}$ vs. $\text{N}@C_{60}$),⁴⁴ the shielding effect from fullerene cage should be completely negligible compared to such a significant weakening effect.

With the above reasons excluded, we conclude that the aggregation of the phthalocyanine moiety in the form of stacking can indirectly decrease the apparent dipolar coupling strength. It has been reported that the CuPc tends to aggregate,^{45,46} and the aggregation in the α phase can lead to the formation of an antiferromagnetic array.^{25,47,48} For the specific CuPc system and experimental conditions discussed in this work, we demonstrated the existence of aggregation effect and its resulting antiferromagnetism by dynamic light scattering (supporting information S6) and EPR analysis of the copper spin (supporting information S7), respectively. Figure 6 compares the dyad molecules in the non-aggregated and aggregated cases. In the non-aggregated case, the standard dipolar coupling will take place and the calculated dipolar coupling strength is feasible. When the CuPc moieties aggregate, the dipolar field of the copper spin experienced by the nitrogen spin in the aggregated case will be significantly suppressed, as the anti-parallel alignment of the copper spins can neutralize the field. Therefore, a weaker apparent dipolar coupling strength can be expected.

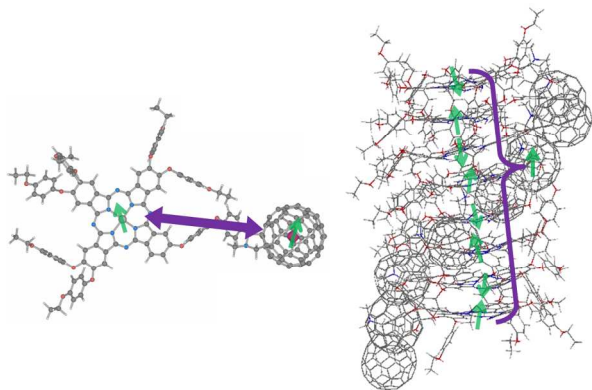


Figure 6. Schematic diagram illustrating the different dipolar coupling strength experienced by the nitrogen spin in the non-aggregated and aggregated cases. (Only one nitrogen spin is expected in the aggregated cluster, due to the 1% endohedral fullerene content in the reagent)

In order to amend the direct simulation model, which is limited to an intramolecular layer and to quantitatively interpret the low coupling strength, the aggregation and antiferromagnetism have to be taken into consideration. However, the weakening effect depends on the size of the aggregation, so it is difficult to individually analyze the varying extent of aggregation in the sample. By observing that the dipolar coupling strength converges to zero as the size of the aggregated cluster grows, we treated the coupling strength as zero in all aggregated cases by a complete suppression approximation. The dipolar field after the neutralization of the antiferromagnetism is negligible compared to that in the non-aggregated case, so

the assumption holds in the majority of cases of the aggregated clusters (see supporting information S8-B). The only considerable coupling strength is in the cluster aggregated by a small number of molecules, but it will merely lead to an insignificant overestimation on the ratio of non-aggregated case to aggregated case, and impose no effect on spectral simulations. Therefore, we combined the spin Hamiltonian model in supporting information S5 with the complete suppression approximation, and did the simulations by fitting the parameter of the aggregation percentage. Figure 7 shows that 75% of non-aggregated case plus 25% of aggregated case was used to fit the spectrum for $\text{N}@C_{60-1}\text{-CuPc}$, and 73% of non-aggregated case plus 27% of aggregated case was used to fit the spectrum for $\text{N}@C_{60-2}\text{-CuPc}$.

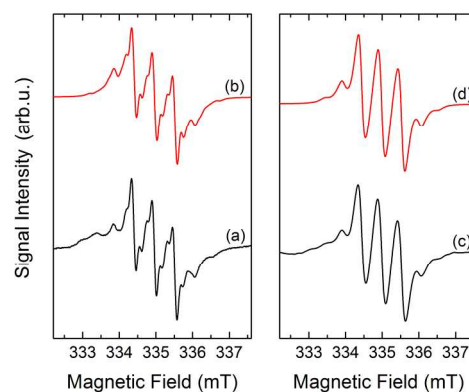


Figure 7. Solid-state CW-EPR spectra for $\text{N}@C_{60-1}\text{-CuPc}$ (a) and $\text{N}@C_{60-2}\text{-CuPc}$ (c), and their corresponding simulation results (b) and (d).

Concentration-dependent dipolar coupling strength

In order to confirm the influence of aggregation to the apparent dipolar coupling strength, and to justify the complete suppression approximation, we measured additional CW-EPR spectra of $\text{N}@C_{60-1}\text{-CuPc}$ in different concentrations, and fitted individual data. All concentration dependent spectra (Figure 8 (a)) were taken with a small microwave power of $3.170 \mu\text{W}$, which maintained linearity of the signal intensity. Therefore the observed spectral variation does not originate from power saturation, but must be caused by the variation of aggregation effect in progressively concentrated samples. Since the dipolar coupling features became more significant when the sample got diluted and less aggregated, we confirmed the suppression effect of the aggregation and its resulting antiferromagnetism on the apparent dipolar coupling strength. The increasing trend of the simulated aggregation percentage (Figure 8 (b)) is consistent with the dynamic light scattering data (supporting information S6) and previously reported results.⁴⁹ Hence, the complete suppression approximation is validated.

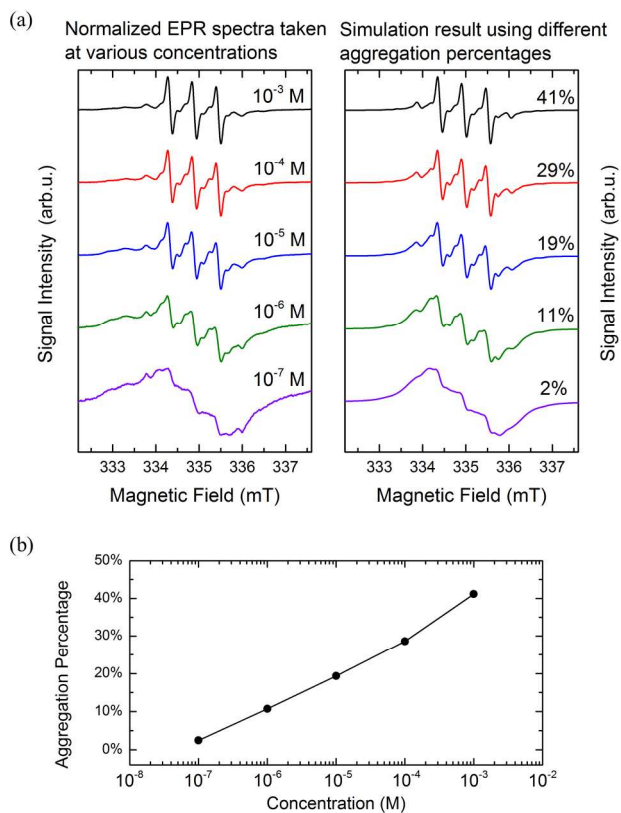


Figure 8. (a) Solid-state CW-EPR spectra for N@C₆₀-1-CuPc frozen toluene solution (100 K) taken at various concentrations, and their corresponding simulation results with different aggregation percentages. (b) Concentration dependence of the aggregation percentage in N@C₆₀-1-CuPc frozen toluene solution sample based on the simulation results.

The solution concentration dependency opens a new way of tuning the dipolar coupling strength in this dyad system. We can turn on the dipolar coupling by diluting the sample, and turn off the dipolar coupling by concentrating the sample, reversibly (supporting information S9). Compared with tuning the dipolar coupling chemically by adjusting the size of the spacer group, changing concentration does not require any change the molecular structure. Since the aggregation effect changes gradually with the concentration, sample concentration cannot enable us to turn on and off the dipolar coupling in a real device. However, if one could adjust the dyad molecules to make the aggregation effect strongly depend on any external stimuli, such as pH, temperature or electric potential, then the control of dipolar coupling could be realized in a device level. Our initial DLS experiment shows that one can change the aggregation properties of the dyad by altering the pH (supporting information S10), but in order to show the spin signal and dipolar coupling features, further confirmation of the comparability between acidic conditions and the endohedral fullerene is required. This is a first step in this direction.

CONCLUSIONS

In summary, we have synthesized three different endohedral fullerene-phthalocyanine dyads. Two of them were

multi-spin systems containing variable spin distances for studying the dipolar coupling, the other one: a dyad with diamagnetic Zn ion worked as the reference. All of the products were characterized by UV-Vis, high resolution MALDI-TOF mass, solution and solid-state CW-EPR. From the solution and solid-state CW-EPR analysis, we determined the spectral features of the dipolar coupling and compared the spectral differences in two dyads having variant spin-spin distance, demonstrating that the chemical adjustment of the spacer group is enough to change the dipolar coupling strength. With the additional discussion of the aggregation and antiferromagnetism of the CuPc moiety, we managed to quantitatively interpret the experimental result with a simulation model, and discovered a new way of tuning the dipolar coupling strength, which utilizes the formation and de-formation of the antiferromagnetic array of CuPc to turn off and turn on the dipolar coupling, respectively.

EXPERIMENTAL SECTION

Preparation of spin enriched N@C₆₀/C₆₀ mixture

As precursors for the endohedral fullerene moieties in the dyads, the mixture of N@C₆₀ in C₆₀ was obtained via an optimized ion implantation procedure.⁵⁹ Its purity was then enhanced from 100 ppm to 1% by recycled HPLC⁵¹⁻⁵³ using 15-PBB and 5-PBB columns by Nacalai Tesque (Japan). All spin percentages were determined by C₆₀ calibrated UV-Vis and TEMPO (2,2,6,6-Tetramethyl-1-piperidinyloxy) calibrated CW-EPR.

Synthesis of phthalocyanine aldehyde

As precursors for the phthalocyanine moieties in the dyads, aldehydes CuPc-1-CHO, CuPc-2-CHO and ZnPc-1-CHO were synthesized through a one-pot reaction with 4,5-bis(4-dodecyloxyphenoxy)phthalonitrile, corresponding central metal ions and 4-(4-formylphenoxy)phthalonitrile (or 4-(4-(4-formylphenoxy)phenoxy)phthalonitrile for the long distanced dyads). The reaction schemes and characterization data for them are listed in supporting information, section S11.

MALDI-TOF

MALDI-TOF measurements were performed with a Bruker Microflex LT spectrometer in positive reflective mode, with Dithranol and CsI₃ as the matrix and the calibration reference, respectively.

CW-EPR

X-Band CW-EPR measurements were performed on a Magnettech Miniscope MS200 and a Bruker EMX spectrometers. Simulations of CW-EPR spectra were performed using the EASYSPPIN software package.⁵⁴

Quantum Chemical Calculations

The geometry optimization and spin distribution calculations were performed with the Gaussian 03 program with an HPC2500 computer at the PM₃ level, followed by the B₃LYP/6-31G(d) level. The frequency analyses were performed at the same level.

ASSOCIATED CONTENT

Supporting Information. The molecular structure of F-C₆₀, the parallel UV/Vis and MS characterizations for N@C₆₀-2-CuPc and N@C₆₀-1-ZnPc, the linewidth comparison of solution EPR spectra, the simulation for frozen N@C₆₀-1-ZnPc toluene solution, the simulation for the multi-spin dyads before the aggregation discussion, the experimental evidence of the aggregation and antiferromagnetism, the synthesis and characterization for the phthalocyanine aldehyde precursors are all reported in the supporting information document. This material is available free of charge via the Internet at <http://pubs.acs.org>.

AUTHOR INFORMATION

Corresponding Author

*kyriakos.porfyarakis@materials.ox.ac.uk

*imahori@scl.kyoto-u.ac.jp

Author Contributions

These authors contributed equally to the experiment.

Notes

The authors declare no competing financial interest.

Funding Sources

This work was supported by EPSRC (EP/K030108/1), a Grant-in-Aid (25620148 to H.I.) and the WPI Initiative of MEXT, Japan.

ACKNOWLEDGMENTS

We thank Yuta Takano, Panagiotis Dallas, Yo Shimizu, and Gregory Rogers for helpful discussions, and Christina Foldbjerg for technical support. We acknowledge CAESR and Dr William Myers for the instrument support during the EPR measurements. S. Z. thanks the National University of Defense Technology and Prof. Haifeng Cheng for the student-ship and support. M. Y. is grateful for a JSPS Fellowship for Young Scientists.

REFERENCES

- Yamada, M.; Kurihara, H.; Suzuki, M.; Saito, M.; Slanina, Z.; Uhlik, F.; Aizawa, T.; Kato, T.; Olmstead, M. M.; Balch, A. L.; Maeda, Y.; Nagase, S.; Lu, X.; Akasaka, T. *J. Am. Chem. Soc.* **2015**, *137*, 232.
- Yamada, M.; Kurihara, H.; Suzuki, M.; Guo, J. D.; Waelchli, M.; Olmstead, M. M.; Balch, A. L.; Nagase, S.; Maeda, Y.; Hasegawa, T.; Lu, X.; Akasaka, T. *J. Am. Chem. Soc.* **2014**, *136*, 7611.
- Popov, A. A.; Pykhova, A. D.; Ioffe, I. N.; Li, F.-F.; Echegoyen, L. *J. Am. Chem. Soc.* **2014**, *136*, 13536.
- Morinaka, Y.; Sato, S.; Wakamiya, A.; Nikawa, H.; Mizorogi, N.; Tanabe, F.; Murata, M.; Komatsu, K.; Furukawa, K.; Kato, T.; Nagase, S.; Akasaka, T.; Murata, Y. *Nat. Commun.* **2013**, *4*, 1554.
- Popov, A. A.; Yang, S.; Dunsch, L. *Chem. Rev.* **2013**, *113*, 5989.
- Lu, X.; Feng, L.; Akasaka, T.; Nagase, S. *Chem. Soc. Rev.* **2012**, *41*, 7649.
- Wang, T.; Wu, J.; Xu, W.; Xiang, J.; Lu, X.; Li, B.; Jiang, L.; Shu, C.; Wang, C. *Angew. Chemie - Int. Ed.* **2010**, *49*, 1786.
- Morton, J. J. L.; Tyryshkin, A. M.; Ardavan, A.; Porfyarakis, K.; Lyon, S. A.; Briggs, G. A. D. *J. Chem. Phys.* **2006**, *124*, 14508.
- Brown, R. M.; Ito, Y.; Warner, J. H.; Ardavan, A.; Shinohara, H.; Briggs, G. A. D.; Morton, J. J. L. *Phys. Rev. B* **2010**, *82*, 033410.
- Harneit, W. *Phys. Rev. A* **2002**, *65*, 032322.
- Benjamin, S. C.; Ardavan, A. *J. Phys. Condens. Matter* **2006**, *18*, S867.
- Wesenberg, J.; Ardavan, A.; Briggs, G.; Morton, J.; Schoelkopf, R.; Schuster, D.; Mølmer, K. *Phys. Rev. Lett.* **2009**, *103*, 070502.
- Yang, W. L.; Xu, Z. Y.; Wei, H.; Feng, M.; Suter, D. *Phys. Rev. A* **2010**, *81*, 032303.
- Plant, S. R.; Jevric, M.; Morton, J. J. L.; Ardavan, A.; Khlobystov, A. N.; Briggs, G. A. D.; Porfyarakis, K. *Chem. Sci.* **2013**, *4*, 2971.
- Feng, M.; Twamley, J. *Phys. Rev. A* **2004**, *70*, 032318.
- Morton, J. J. L.; Tyryshkin, A. M.; Ardavan, A.; Porfyarakis, K.; Lyon, S. a.; Briggs, G. A. D. *Phys. Rev. Lett.* **2005**, *95*, 1.
- Ju, C.; Suter, D.; Du, J. *Phys. Lett. A* **2011**, *375*, 1441.
- Morton, J. J. L.; Tyryshkin, A. M.; Ardavan, A.; Benjamin, S. C.; Porfyarakis, K.; Lyon, S. A.; Briggs, G. A. D. *Nat. Phys.* **2006**, *2*, 40.
- Filidou, V.; Simmons, S.; Karlen, S. D.; Giustino, F.; Anderson, H. L.; Morton, J. J. L. *Nat. Phys.* **2012**, *8*, 596.
- Ju, C.; Suter, D.; Du, J. *Phys. Rev. A* **2007**, *75*, 012318.
- Liu, G.; Khlobystov, A. N.; Charalambidis, G.; Coutsolelos, A. G.; Briggs, G. A. D.; Porfyarakis, K. *J. Am. Chem. Soc.* **2012**, *134*, 1938.
- Wu, B.; Wang, T.; Feng, Y.; Zhang, Z.; Jiang, L.; Wang, C. *Nat. Commun.* **2015**, *6*, 6468.
- Farrington, B. J.; Jevric, M.; Rance, G. A.; Ardavan, A.; Khlobystov, A. N.; Briggs, G. A. D.; Porfyarakis, K. *Angew. Chem. Int. Ed.* **2012**, *51*, 3587.
- Warner, M.; Din, S.; Tupitsyn, I. S.; Morley, G. W.; Stoneham, a M.; Gardener, J. a; Wu, Z.; Fisher, A. J.; Heutz, S.; Kay, C. W. M.; Aeppli, G. *Nature* **2013**, *503*, 504.
- Wang, H.; Mauthoor, S.; Din, S.; Gardener, J. a.; Chang, R.; Warner, M.; Aeppli, G.; McComb, D. W.; Ryan, M. P.; Wu, W.; Fisher, A. J.; Stoneham, M.; Heutz, S. *ACS Nano* **2010**, *4*, 3921.
- Hayashi, H.; Nihashi, W.; Umeyama, T.; Matano, Y.; Seki, S.; Shimizu, Y.; Imahori, H. *J. Am. Chem. Soc.* **2011**, *133*, 10736.
- Maggini, M.; Scorrano, G.; Prato, M. *J. Am. Chem. Soc.* **1993**, *115*, 9798.
- Prato, M.; Maggini, M. *Acc. Chem. Res.* **1998**, *31*, 519.
- Waiblinger, M.; Lips, K.; Harneit, W.; Weidinger, A.; Dietel, E.; Hirsch, A. *Phys. Rev. B* **2001**, *64*, 159901.
- Liu, G.; Khlobystov, A. N.; Ardavan, A.; Briggs, G. A. D.; Porfyarakis, K. *Chem. Phys. Lett.* **2011**, *508*, 187.
- Zhou, S.; Rašović, I.; Briggs, G. A. D.; Porfyarakis, K. *Chem. Commun.* **2015**, *51*, 7096.
- Imahori, H.; Ozawa, S.; Ushida, K.; Takahashi, M.; Azuma, T.; Ajavakom, A.; Akiyama, T.; Hasegawa, M.; Taniguchi, S.; Okada, T.; Sakata, Y. *Bull. Chem. Soc. Jpn.* **1999**, *72*, 485.
- Bensasson, R. V.; Bienvenüe, E.; Fabre, C.; Janot, J. M.; Land, E. J.; Leach, S.; Leboulaire, V.; Rassat, A.; Roux, S.; Seta, P. *Chem. Eur. J.* **1998**, *4*, 270.
- Shultz, D. A.; Mussari, C. P.; Ramanathan, K. K.; Kampf, J. W. *Inorg. Chem.* **2006**, *45*, 5752.

- 1
2
3
4
5
6
7
8
9
10
11
12
13
14
15
16
17
18
19
20
21
22
23
24
25
26
27
28
29
30
31
32
33
34
35
36
37
38
39
40
41
42
43
44
45
46
47
48
49
50
51
52
53
54
55
56
57
58
59
60
- (35) Shultz, D. A.; Fico, R. M.; Bodnar, S. H.; Kumar, R. K.; Vostrikova, K. E.; Kampf, J. W.; Boyle, P. D. *J. Am. Chem. Soc.* **2003**, *125*, 11761.
- (36) Ayabe, K.; Sato, K.; Nishida, S.; Ise, T.; Nakazawa, S.; Sugisaki, K.; Morita, Y.; Toyota, K.; Shiomi, D.; Kitagawa, M.; Takui, T. *Phys. Chem. Chem. Phys.* **2012**, *14*, 9137.
- (37) Knapp, C.; Dinse, K. P.; Pietzak, B.; Waiblinger, M.; Weidinger, A. *Chem. Phys. Lett.* **1997**, *272*, 433.
- (38) Zhang, J.; Morton, J. J. L.; Sambrook, M. R.; Porfyrakis, K.; Ardavan, A.; Briggs, G. A. D. *Chem. Phys. Lett.* **2006**, *432*, 523.
- (39) Morton, J. J. L.; Tyryshkin, A. M.; Ardavan, A.; Porfyrakis, K.; Lyon, S. a.; Briggs, G. A. D. *Phys. Rev. B* **2007**, *76*, 085418.
- (40) Goedde, B.; Waiblinger, M.; Jakes, P.; Weiden, N.; Dinse, K. P.; Weidinger, A. *Chem. Phys. Lett.* **2001**, *334*, 12.
- (41) Franco, L.; Ceola, S.; Corvaja, C.; Bolzonella, S.; Harneit, W.; Maggini, M. *Chem. Phys. Lett.* **2006**, *422*, 100.
- (42) Banham, J. E.; Baker, C. M.; Ceola, S.; Day, I. J.; Grant, G. H.; Groenen, E. J. J.; Rodgers, C. T.; Jeschke, G.; Timmel, C. R. *J. Magn. Reson.* **2008**, *191*, 202.
- (43) Saunders, M.; Jiménez-Vázquez, H. A.; Cross, R. J.; Mroczkowski, S.; Freedberg, D. I.; Anet, F. A. L. *Nature* **1994**, *367*, 256.
- (44) Lips, K.; Waiblinger, M.; Pietzak, B.; Weidinger, A. *Phys. Status Solidi A* **2000**, *177*, 81.
- (45) Monahan, A. R.; Brado, J. A.; DeLuca, A. F. *J. Phys. Chem.* **1972**, *76*, 446.
- (46) Monahan, A. R.; Brado, J. A.; DeLuca, A. F. *J. Phys. Chem.* **1972**, *76*, 1994.
- (47) Serri, M.; Wu, W.; Fleet, L. R.; Harrison, N. M.; Hirjibehedin, C. F.; Kay, C. W. M.; Fisher, A. J.; Aeppli, G.; Heutz, S. *Nat. Commun.* **2014**, *5*, 3079.
- (48) Heutz, S.; Mitra, C.; Wu, W.; Fisher, A. J.; Kerridge, A.; Stoneham, M.; Harker, T. H.; Gardener, J.; Tseng, H. H.; Jones, T. S.; Renner, C.; Aeppli, G. *Adv. Mater.* **2007**, *19*, 3618.
- (49) Camp, P. J.; Jones, A. C.; Neely, R. K.; Speirs, N. M. *J. Phys. Chem. A* **2002**, *106*, 10725.
- (50) Murphy, T. A.; Pawlik, T.; Weidinger, A.; Höhne, M.; Alcalá, R.; Spaeth, J. M. *Phys. Rev. Lett.* **1996**, *77*, 1075.
- (51) Kanai, M.; Porfyrakis, K.; Briggs, G. A. D.; Dennis, T. J. S. *Chem. Commun.* **2004**, *40*, 210.
- (52) Jakes, P.; Dinse, K. P.; Meyer, C.; Harneit, W.; Weidinger, A. *Phys. Chem. Chem. Phys.* **2003**, *5*, 4080.
- (53) Plant, S. R.; Porfyrakis, K. *Analyst* **2014**, *139*, 4519.
- (54) Stoll, S.; Schweiger, A. *J. Magn. Reson.* **2006**, *178*, 42.

TOC

